COBEM 99
XV Congresso Brasileiro de Engenharia Mecânica
15th Brazilian Congress of Mechanical Engineering
22 - 26 de Novembro de 1999 / November 22 - 26, 1999 Águas de Lindóia, São Paulo,

# BOUNDS FOR THE EFFECTIVE CONDUCTIVITY OF UNIDIRECTIONAL COMPOSITES BASED ON ISOTROPIC MICROSCALE MODELS

**Leandro B. Machado**
**Manuel E. Cruz**
Federal University of Rio de Janeiro, EE/COPPE, Department of Mechanical Engineering
Cx. P. 68503 - 21945-970 — Rio de Janeiro, RJ, Brazil
e-mail: manuel@serv.com.ufrj.br

***Abstract.*** *The numerical study of heat conduction in composite materials is much adversely affected by the geometrical stiffness arising from their generally complex microstructures, particularly at high concentrations. With the purpose of alleviating the consequences of geometrical stiffness, in this paper we develop bounds for the effective conductivity of unidirectional composites with a thermally-conducting dispersed phase, based on simple isotropic microscale models. Our approach proceeds by an inner-outer decomposition, in which analytical approximations at the microscale are folded into modified outer problems defined over geometrically more homogeneous domains. Rigorous lower and upper bounds for the effective conductivity are then defined based on the solutions of these outer problems. The bounds are motivated physically and proven mathematically, by using classical variational space restriction and embedding arguments. The formulation is applicable to both ordered and random fibrous composites, and it is easily extendable to three-dimensional particulate composites.*

***Keywords:*** *Heat Conduction; Variational Bounds; Composites; Effective Conductivity*

## 1. INTRODUCTION

Composite materials are engineered to attain a wide range of mechanical and thermal macroscopic properties, at a lower cost and higher efficiency as compared to the individual components. The determination of macroscopic, or effective, properties of composites, in terms of the microstructure and component properties, is thus of fundamental and practical importance. For the heat conduction problem in thermal composite materials, many different approaches have been adopted to determine the effective conductivity: statistical microstructure-independent bound methods (Torquato, 1991), cell-model semi-analytical treatments (Sangani & Yao, 1988; Perrins *et al.*, 1979), phenomenological modelling (Tzou, 1991), computational procedures (Cruz & Patera, 1995; Ghaddar, 1994), and experimental studies (Hasselman *et al.*, 1987; Pilling *et al.*, 1979). Recent reviews of the subject of heat conduction in composites are presented in Ayers & Fletcher (1998) and Furmański (1997).

An important class of problems of heat conduction in composite materials is the transverse conduction in fibrous composites, in particular the ones composed of monodisperse unidirectional solid circular fibers distributed in a continuous matrix (Furmañski, 1997). The positions of the cylinders, or fibers, may be orderly or randomly distributed in space. For such composites, rigorous (transverse) effective conductivity results for which precise error bounds are known, are still needed in the practically–relevant range of concentration values (or fiber volume fractions) corresponding to medium to highly–packed media (Hasselman *et al.*, 1987; Pilling *et al.*, 1979). The semi–analytical series expansion techniques to calculate the effective conductivity of *ordered* (Perrins *et al.*, 1979) and *random* fiber arrays (Sangani & Yao, 1988) have serious convergence and error control problems when maximum packing is approached, particularly for higher values of the conductivity of the fibers.

Although better suited than analytical and semi–analytical approaches to treat complex geometries and nonlinear phenomena, finite–element based computational procedures (Cruz & Patera, 1995) suffer from the severe geometric stiffness which arises when treating the distorted domains associated with randomly–arranged, medium to highly–packed fibers. The boundaries of very close fibers form nip regions, or nips, that may be hard, or even impossible, to mesh, rendering numerical solutions either prohibitively expensive, due to excessive degrees–of–freedom and ill–conditioning, or hopeless. Ghaddar (1994) and Cruz *et al.* (1995) developed a variational–bound nip–element methodology to alleviate the problems caused by geometric stiffness, and applied the technique to the practically–limited problem of heat conduction in composites with an *insulating* dispersed phase. The hybrid analytico–computational methodology is rigorously applicable to problems for which the effective property of interest is the extremum of a quadratic, symmetric, positive–definite functional. The approach proceeds by an inner–outer decomposition of the geometrically stiff problem, in which analytical approximations in inner nip regions — the *microscale models* — are folded into a modified outer problem defined over a geometrically more homogeneous domain. As a result, by virtue of the variational nature of the problem, rigorous upper and lower bounds for the effective property may be designed.

In this paper, we extend the variational–bound nip–element technique to solve the problem of transverse heat conduction in unidirectional composites with a *thermally–conducting* dispersed phase; to construct the bounds, we employ simple isotropic microscale models. The composite medium is periodic, and we assume a perfect thermal contact between the constituent phases. Our continuous and numerical formulations are applicable to both ordered and random fibrous composites; with the purpose of illustrating the capabilities of our approach, here we compute the transverse effective conductivity for the square array of fibers at high concentrations, including maximum packing. Future work shall employ more sophisticated and accurate anisotropic microscale models (Cruz *et al.*, 1995; Ghaddar, 1994) in a more complete study of heat conduction in *random* fibrous composites; such study is more relevant to practical applications, and it *necessitates* the bounding procedure developed here.

## 2. HEAT CONDUCTION IN UNIDIRECTIONAL COMPOSITES WITH A THERMALLY–CONDUCTING DISPERSED PHASE

We consider heat conduction in a unidirectional periodic composite medium, $\Omega$, composed of monodisperse co–oriented circular cylindrical fibers of thermal conductivity $k_d$ dispersed in a continuous matrix of thermal conductivity $k_c$; we define $\alpha \equiv k_d/k_c$, $k_c > 0$. It is assumed that the components have a perfect thermal contact, and are solid, homogeneous, and isotropic. The geometric regions occupied by the continuous and dispersed components are, respectively, $\Omega_c$ and $\Omega_d$. An external transverse temperature gradient of magnitude $\Delta T/L$ is imposed over the *macroscale* $L$ of $\Omega$. The smallest scale of $\Omega$ is the diameter of the dispersed fibers, $d$, called the *microscale*. The *mesoscale* $\lambda$ ($d < \lambda \ll L$) is the characteristic size of the periodic cell, $\Omega_{pc}$, of area $\lambda^2$, which contains $N$ fibers; the concentration is thus given by $c = N\pi d^2/4\lambda^2$.

In Cruz and Patera (1995), a variational hierarchical scale–decoupling procedure for random media is described, which decomposes the original multiscale problem in $\Omega$ into the microscale (length scale $d$), mesoscale (length scale $\lambda$), and macroscale (length scale $L$) problems. In the macroscale problem, the effective conductivity is used (input) in the energy equation to calculate the bulk heat flow rate through the homogenized medium. In the mesoscale problem, the effective conductivity is determined (output), by solving an appropriate sequence of periodic–cell problems generated in a Monte–Carlo loop. Finally, in the microscale problem (see section 3), the nearfield behavior of nip–forming fibers is modeled and subsequently incorporated into the mesoscale problem.

For the purposes of this paper, we are interested in the microscale–prepared mesoscale cell problem; specifically, we want to determine the effective conductivity of particular cell configurations, or realizations, of the composite medium which contain one or more pairs of close fibers forming nip regions. Such configurations are more likely to occur at higher concentrations. We thus need, first, the formulation of the transverse heat conduction mesoscale problem in $\Omega_{pc}$, which is obtained from the original multiscale problem in $\Omega$ by applying the method of homogenization (Cruz, 1997; Furmañski, 1997). From Cruz (1997), we know that the non–dimensional weak form of the cell problem for an *isotropic* composite medium takes the form (using $d$ and $\Delta T(d/L)$ as the characteristic length and temperature scales, respectively)

$$\int_{\Omega_{pc,c}} \frac{\partial \chi^c}{\partial y_j}\frac{\partial v^c}{\partial y_j}\,d\mathbf{y} + \int_{\Omega_{pc,d}} \alpha\,\frac{\partial \chi^d}{\partial y_j}\frac{\partial v^d}{\partial y_j}\,d\mathbf{y} = \int_{\Omega_{pc,c}} \frac{\partial v^c}{\partial y_1}\,d\mathbf{y} + \int_{\Omega_{pc,d}} \alpha\,\frac{\partial v^d}{\partial y_1}\,d\mathbf{y} \quad \forall v \in Y(\Omega_{pc})\,, \quad (1)$$

where: $\chi$ is the mesoscale temperature perturbation, and $\chi^c = \chi_{|\Omega_{pc,c}}$ and $\chi^d = \chi_{|\Omega_{pc,d}}$; $(y_1, y_2) = \mathbf{y}$ are the space coordinates, and $d\mathbf{y} = dy_1 dy_2$; $\Omega_{pc,c}$ and $\Omega_{pc,d}$ are, respectively, the portions of $\Omega_{pc}$ in the continuous and dispersed components; $Y(\Omega_{pc}) = \{w \in H^1_{\#}(\Omega_{pc}) \,|\, w_{|\Omega_{pc,c}} = w^c, w_{|\Omega_{pc,d}} = w^d, \int_{\Omega_{pc,c}} w^c\,d\mathbf{y} + \int_{\Omega_{pc,d}} w^d\,d\mathbf{y} = 0\}$, $H^1_{\#}(\Omega_{pc})$ is the space of all $\lambda$–doubly periodic functions in $\Omega_{pc}$ for which both the function and derivative are square–integrable over $\Omega_{pc}$; and the external temperature gradient is (arbitrarily) set in the $y_1$ direction. Problem (1) has been solved in Cruz (1997) for ordered composites, for various values of the concentration; however, due to the lack of the microscale preparation, Cruz (1997) was unable to approach maximum packing.

The microscale bounds that we shall here develop, are based on the equivalent variational form of problem (1), given by

$$\chi = \arg \min_{w \in Y(\Omega_{pc})} J_{\Omega_{pc}}(w)\,, \quad (2)$$

where the functional $J_{\Omega_{pc}}$ is defined by

$$J_{\Omega_{pc}}(w) = \int_{\Omega_{pc,c}} \frac{\partial w^c}{\partial y_j}\frac{\partial w^c}{\partial y_j}\,d\mathbf{y} + \int_{\Omega_{pc,d}} \alpha\,\frac{\partial w^d}{\partial y_j}\frac{\partial w^d}{\partial y_j}\,d\mathbf{y} - 2\left(\int_{\Omega_{pc,c}} \frac{\partial w^c}{\partial y_1}\,d\mathbf{y} + \int_{\Omega_{pc,d}} \alpha\,\frac{\partial w^d}{\partial y_1}\,d\mathbf{y}\right). \quad (3)$$

Clearly, the weak form (1) for $\chi$ derives from the first variation of the functional $J_{\Omega_{pc}}$, which must be zero at $w = \chi$.

Once the mesoscale temperature field $\chi$ of Eq. (1) (or Eq. (2)) has been found for the particular cell configuration of the composite medium, the corresponding *transverse effective thermal conductivity*, $k_e$, can be computed from the expression (Cruz, 1997)

$$k_e = \frac{1}{|\Omega_{pc}|}\left(\int_{\Omega_{pc,c}} \left[1 - \frac{\partial \chi^c}{\partial y_1}\right] d\mathbf{y} + \int_{\Omega_{pc,d}} \alpha \left[1 - \frac{\partial \chi^d}{\partial y_1}\right] d\mathbf{y}\right)\,, \quad (4)$$

where, by isotropy, $k_e$ is scalar, $|\Omega_{pc}| \equiv \int_{\Omega_{pc}} d\mathbf{y} = \lambda^2/d^2$ is the non–dimensional area of the periodic cell, and $k_e$ is non–dimensionalized with respect to $k_c$. Manipulating Eqs. (1)–(4),

it can easily be shown that $k_e$ satisfies the following minimization principle (Machado, 1999), which is essential for constructing the microscale bounds presented in the next section:

$$k_e \;=\; \min_{w \,\in\, Y(\Omega_{pc})} a_{\Omega_{pc}}(w) \;=\; a_{\Omega_{pc}}(\chi)\,, \tag{5}$$

where $a_\sigma(w)$ is the quadratic form

$$a_\sigma(w) \;=\; \frac{1}{|\Omega_{pc}|}\left(\int_{\sigma_c}\left[\frac{\partial}{\partial y_j}(y_1 - w)\right]^2 d\mathbf{y} \;+\; \int_{\sigma_d}\alpha\left[\frac{\partial}{\partial y_j}(y_1 - w)\right]^2 d\mathbf{y}\right)\,, \tag{6}$$

$\sigma_c$ and $\sigma_d$ are, respectively, the portions of $\sigma \subseteq \Omega_{pc}$ in the continuous and dispersed components.

## 3. MICROSCALE VARIATIONAL BOUNDS

In Cruz *et al.* (1995) and Ghaddar (1994), the microscale component of the macro–meso–microscale formulation of Cruz & Patera (1995) is described and discussed in detail. Our purpose here is to formulate isotropic microscale models to avoid the nip regions between close fibers which preclude mesh generation. In this section we present and apply such nip–region models to the heat conduction problem in unidirectional composites with a thermally–conducting dispersed phase; the models lead to lower and upper bounds for the effective conductivity $k_e$. The bounds rely on the minimization property, Eq. (5), of $k_e$. The variational forms of the microscale–prepared mesoscale problems associated with the lower and upper bounds resemble Eq. (2), and are respectively defined over the modified ('less stiff') domains $\mathcal{L}$ and $\mathcal{U}$, as shown below.

### 3.1. Nips Geometries

The geometries of the nip regions for the lower and upper bounds are shown in Figure 1. As the concentration increases, it is more likely that one fiber in a cell will get very close to other fibers in the same cell or in neighboring cells; we postulate that a pair of close fibers forms a nip when the center–to–center (nondimensional) separation distance $1+\gamma$ is less than $1+\gamma_c$, where $\gamma_c$ is a (small) prescribed parameter. For the lower, Figure 1(a), and upper, Figure 1(b), bounds, we respectively define: $\mathcal{D}_{\mathrm{LB},n}$ and $\mathcal{D}_{\mathrm{UB},n}$ are the domains associated with nip region $n$, $n = 1,\ldots,\mathcal{N}$, $\mathcal{N}$ is the number of nips in the cell; $\mathcal{L} = \Omega_{pc}\setminus\cup_{n=1}^{\mathcal{N}}\mathcal{D}_{\mathrm{LB},n}$ and $\mathcal{U} = \Omega_{pc}\setminus\cup_{n=1}^{\mathcal{N}}\mathcal{D}_{\mathrm{UB},n}$ are the associated modified mesoscale cell domains; and $\beta$ is half the distance between the edges of $\mathcal{D}_{\mathrm{LB},n}$ or $\mathcal{D}_{\mathrm{UB},n}$ parallel to the line joining the fibers centers.

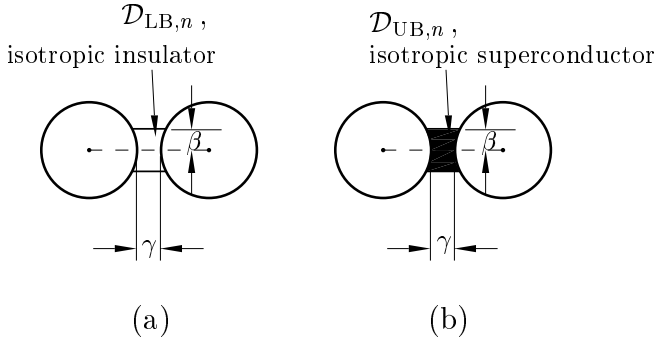


Figure 1: (a) Geometry of one lower–bound nip region, $\mathcal{D}_{\mathrm{LB},n}$. (b) Geometry of one upper–bound nip region, $\mathcal{D}_{\mathrm{UB},n}$.

In the next two subsections, we employ isotropic microscale models to construct rigorous lower and upper bounds for the effective conductivity, $k_{\mathrm{LB}} \le k_e \le k_{\mathrm{UB}}$, based only on solutions defined over $\mathcal{L}$ and $\mathcal{U}$, respectively: we avoid the hard– or impossible–to–mesh nip regions, while maintaining strict control over the resulting error.

### 3.2. Lower Bound

A lower bound for $k_e$ , $k_{\rm LB}$ , can be obtained by simply assuming that the material in the nip regions $\mathcal{D}_{{\rm LB},n}$ , $n = 1,\ldots,\mathcal{N}$, is an *isotropic insulator*; thus, since the total available area for transverse heat flow is decreased, we physically expect $k_{\rm LB}$ to be a lower bound. Because the thermal conductivity is zero inside the nips, the inner problems in $\cup_{n=1}^{\mathcal{N}}\mathcal{D}_{{\rm LB},n}$ are irrelevant. The lower bound $k_{\rm LB}$ will depend on the temperature field $\chi_{\rm LB}$ inside the modified cell domain $\mathcal{L} = \mathcal{L}_c \cup \Omega_{pc,d}$ , $\mathcal{L}_c = \Omega_{pc,c} \setminus \cup_{n=1}^{\mathcal{N}}\mathcal{D}_{{\rm LB},n}$ , which is given by the variational form

$$\chi_{\rm LB} \;=\; \arg \min_{w \,\in\, X_{\#,{\rm LB}}(\mathcal{L})} J_{\mathcal{L}}(w)\,, \tag{7}$$

where $X_{\#,{\rm LB}}(\mathcal{L}) = \{w \in H^1_{\#}(\mathcal{L}) \,|\, w_{|_{\mathcal{L}_c}} = w^c, w_{|_{\Omega_{pc,d}}} = w^d, \int_{\mathcal{L}_c} w^c\, d\mathbf{y} + \int_{\Omega_{pc,d}} w^d\, d\mathbf{y} \;=\; 0\}$. From Eq. (3), we write $J_{\mathcal{L}}(w)$ as

$$J_{\mathcal{L}}(w) \;=\; \int_{\mathcal{L}_c} \frac{\partial w^c}{\partial y_j}\frac{\partial w^c}{\partial y_j}\, d\mathbf{y} \;+ \int_{\Omega_{pc,d}} \alpha\, \frac{\partial w^d}{\partial y_j}\frac{\partial w^d}{\partial y_j}\, d\mathbf{y} - 2\left(\int_{\mathcal{L}_c} \frac{\partial w^c}{\partial y_1}\, d\mathbf{y} \;+ \int_{\Omega_{pc,d}} \alpha\, \frac{\partial w^d}{\partial y_1}\, d\mathbf{y}\right)\,. \tag{8}$$

Therefore, from the first variation of $J_{\mathcal{L}}(w)$ we derive the weak form for the field of the microscale–prepared mesoscale lower–bound problem: Find $\chi_{\rm LB} \in X_{\#,{\rm LB}}(\mathcal{L})$ such that, $\forall v \in X_{\#,{\rm LB}}(\mathcal{L})$,

$$\int_{\mathcal{L}_c} \frac{\partial \chi^c_{\rm LB}}{\partial y_j}\frac{\partial v^c}{\partial y_j}\, d\mathbf{y} \;+ \int_{\Omega_{pc,d}} \alpha\, \frac{\partial \chi^d_{\rm LB}}{\partial y_j}\frac{\partial v^d}{\partial y_j}\, d\mathbf{y} \;=\; \int_{\mathcal{L}_c} \frac{\partial v^c}{\partial y_1}\, d\mathbf{y} \;+ \int_{\Omega_{pc,d}} \alpha\, \frac{\partial v^d}{\partial y_1}\, d\mathbf{y}\,. \tag{9}$$

The main difference of problem (9) with respect to the original problem (1) is that $\mathcal{L}_c$ in the former substitutes $\Omega_{pc,c}$ in the latter. Equation (9) naturally enforces the appropriate Neumann boundary conditions on $\chi_{\rm LB}$ at the straight and curved segments of each insulating nip region, such that the global (macroscopic) heat flux is zero at these segments.

In view of the results in the previous section for the effective conductivity $k_e$ , we now define, based on the solution $\chi_{\rm LB}$ of the modified problem (9) in $\mathcal{L}$, the quantity $k_{\rm LB}$ as

$$k_{\rm LB} \;\equiv\; a_{\mathcal{L}}(\chi_{\rm LB})\,, \tag{10}$$

which is shown below to be a lower bound for $k_e$ . From Eqs. (7)–(10) and (6), it follows that (Machado, 1999)

$$k_{\rm LB} \;=\; \min_{w \,\in\, X_{\#,{\rm LB}}(\mathcal{L})} a_{\mathcal{L}}(w)\,. \tag{11}$$

Also, from Eqs. (9)–(10) and (6), we can rewrite $k_{\rm LB}$ as

$$k_{\rm LB} \;=\; (1-\tilde{c}) + \alpha c \;-\; \frac{1}{|\Omega_{pc}|}\left(\int_{\mathcal{L}_c} \frac{\partial \chi^c_{\rm LB}}{\partial y_1}\, d\mathbf{y} \;+ \int_{\Omega_{pc,d}} \alpha\, \frac{\partial \chi^d_{\rm LB}}{\partial y_1}\, d\mathbf{y}\right)\,, \tag{12}$$

where $\tilde{c}$ is an 'effective concentration' given by $\tilde{c} \;=\; 1 - (1/|\Omega_{pc}|)\int_{\mathcal{L}_c} d\mathbf{y}$.

Finally, we now prove mathematically the physically–expected bounding property of $k_{\rm LB}$ , by using domain embedding arguments:

$$\begin{aligned} k_{\rm LB} \;=\; a_{\mathcal{L}}(\chi_{\rm LB}) \;&=\; \min_{w \,\in\, X_{\#,{\rm LB}}(\mathcal{L})} a_{\mathcal{L}}(w) \\ &\leq\; a_{\mathcal{L}}(\chi_{|_{\mathcal{L}}} + s) \;=\; a_{\mathcal{L}}(\chi_{|_{\mathcal{L}}}) \qquad (13) \\ &\leq\; a_{\Omega_{pc}}(\chi) \;=\; k_e\,. \qquad (14) \end{aligned}$$

In (13), $\chi_{|_{\mathcal{L}}}$ is the solution to the original mesoscale problem (1) restricted to $\mathcal{L}$, and $s \in \mathbb{R}$ is the required shift such that $\int_{\mathcal{L}}(\chi_{|_{\mathcal{L}}} + s)d\mathbf{y} = 0$. The inequality (13) follows from the fact that $(\chi_{|_{\mathcal{L}}} + s) \in X_{\#,{\rm LB}}(\mathcal{L})$; the inequality (14) follows from the positive–(semi)definiteness of the quadratic form defined in Eq. (6), which leads to a positive contribution over $\Omega_{pc} \setminus \mathcal{L}$.

### 3.3. Upper Bound

An upper bound for $k_e$, $k_{\rm UB}$, can be obtained by simply assuming that the material in the nip regions $\mathcal{D}_{{\rm UB},n}$, $n = 1,\ldots,\mathcal{N}$, is an *isotropic superconductor*; thus, since the total capacity for transverse heat flow is increased, we physically expect $k_{\rm UB}$ to be an upper bound. Because the thermal conductivity is infinite inside the nip regions, the inner problems in $\cup_{n=1}^{\mathcal{N}}\mathcal{D}_{{\rm UB},n}$ have trivial solutions: the nips are isothermal, so that the temperature field $\chi_{\rm UB}$ over the cell domain $\Omega_{pc}$ is constant inside each superconducting nip. The upper bound $k_{\rm UB}$ will depend on $\chi_{\rm UB}$, whose variational form is

$$\chi_{\rm UB} \;=\; \arg \min_{w\,\in\, W_{\#,{\rm UB}}(\Omega_{pc})} J_{\Omega_{pc}}(w)\,, \tag{15}$$

where $W_{\#,{\rm UB}}(\Omega_{pc}) = \{w \in H^1_{\#}(\Omega_{pc}) \,|\, w_{|_{\mathcal{U}_c}} = w^c, w_{|_{\Omega_{pc,d}}} = w^d, w_{|_{\mathcal{D}_{{\rm UB},n}}} = C_n\,, n = 1,\ldots,\mathcal{N}\,,$ $\int_{\Omega_{pc}} w\,d\mathbf{y} = 0\}$, $C_n \in I\!R$ part of the solution, and $\mathcal{U}$ is the modified cell domain, $\mathcal{U} = \mathcal{U}_c \cup \Omega_{pc,d}$, $\mathcal{U}_c = \Omega_{pc,c} \setminus \cup_{n=1}^{\mathcal{N}}\mathcal{D}_{{\rm UB},n}$; it is important to note that $W_{\#,{\rm UB}}(\Omega_{pc}) \subset Y(\Omega_{pc})$ (function space restriction). We can express the functional $J_{\Omega_{pc}}(w)$ as

$$J_{\Omega_{pc}}(w) \;=\; J_{\mathcal{U}}(w_{|_{\mathcal{U}}}) \;+\; \sum_{n=1}^{\mathcal{N}} J_{\mathcal{D}_{{\rm UB},n}}(w_{|_{\mathcal{D}_{{\rm UB},n}}})\,, \tag{16}$$

where $w_{|_{\mathcal{U}}}$ and $w_{|_{\mathcal{D}_{{\rm UB},n}}}$ are the restrictions of $w(\mathbf{y})$ to $\mathcal{U}$ and $\mathcal{D}_{{\rm UB},n}$, respectively.

We can now break the problem (15) into $\mathcal{N}$ inner (microscale) problems defined over the nip regions,

$$\chi_{{\rm UB,in}}\{\mathbf{y};\overline{C}_n\} \;=\; \arg \min_{w\,\in\, W_{\rm UB}(\mathcal{D}_{{\rm UB},n})} J_{\mathcal{D}_{{\rm UB},n}}(w)\,, \quad n = 1,\ldots,\mathcal{N}\,, \tag{17}$$

and an outer problem defined over $\mathcal{U}$,

$$\chi_{\rm UB,out} \;=\; \arg \min_{w\,\in\, \overline{W}_{\#,{\rm UB}}(\mathcal{U})} \left( J_{\mathcal{U}}(w) + \sum_{n=1}^{\mathcal{N}} J_{\mathcal{D}_{{\rm UB},n}}(\chi_{{\rm UB,in}}\{\mathbf{y}; w_{|_{\partial\mathcal{D}_{{\rm UB},n}}}\}) \right)\,, \tag{18}$$

where: $W_{\rm UB}(\mathcal{D}_{{\rm UB},n})$ is the rather trivial set of all functions $w(\mathbf{y}) \in H^1(\mathcal{D}_{{\rm UB},n})$ for which $w = \overline{C}_n$, $\overline{C}_n \in I\!R$ *given* (inner: nips are isothermal); $\overline{W}_{\#,{\rm UB}}(\mathcal{U}) = \{w \in H^1_{\#}(\mathcal{U}) \,|\, w_{|_{\mathcal{U}_c}} = w^c, w_{|_{\Omega_{pc,d}}} = w^d, w_{|_{\partial\mathcal{D}_{{\rm UB},n}}} = C_n\,, n = 1,\ldots,\mathcal{N},\ \int_{\mathcal{U}} w\,d\mathbf{y} = 0\}$, $C_n \in I\!R$ *part* of the (outer) solution; $\partial\mathcal{D}_{{\rm UB},n}$ is the boundary of nip $\mathcal{D}_{{\rm UB},n}$, composed of the two straight edges and two arcs of circle (see Figure 1(b)); and

$$\chi_{\rm UB,out} \;=\; \chi_{\rm UB}|_{\mathcal{U}} + s'\,, \qquad \chi_{{\rm UB,in}}\{\mathbf{y}; \chi_{\rm UB,out}|_{\partial\mathcal{D}_{{\rm UB},n}}\} \;=\; \chi_{\rm UB}|_{\mathcal{D}_{{\rm UB},n}} + s'\,, \quad n = 1,\ldots,\mathcal{N}\,, \tag{19}$$

$s' \in I\!R$ is a constant shift such that $\int_{\Omega_{pc}} \chi_{\rm UB}\,d\mathbf{y} = 0$ and $\int_{\mathcal{U}} \chi_{\rm UB,out}\,d\mathbf{y} = 0$ may be obtained.

The inner problems have trivial solutions in this case, since by assumption $\chi_{{\rm UB,in}}\{\mathbf{y};\overline{C}_n\} = \overline{C}_n$, $n = 1,\ldots,\mathcal{N}$. The outer problem thus becomes

$$\chi_{\rm UB,out} \;=\; \arg \min_{w\,\in\, \overline{W}_{\#,{\rm UB}}(\mathcal{U})} J_{\mathcal{U}}(w)\,, \tag{20}$$

since $J_{\mathcal{D}_{{\rm UB},n}}(\chi_{{\rm UB,in}}\{\mathbf{y};\overline{C}_n\}) = 0$, $n = 1,\ldots,\mathcal{N}$. Taking the first variation of $J_{\mathcal{U}}(w)$, we obtain the weak form for the field of the microscale–prepared mesoscale upper–bound problem: Find $\chi_{\rm UB,out} \in \overline{W}_{\#,{\rm UB}}(\mathcal{U})$ such that, $\forall v \in \overline{W}_{\#,{\rm UB}}(\mathcal{U})$,

$$\int_{\mathcal{U}_c} \frac{\partial\chi^c_{\rm UB,out}}{\partial y_j}\frac{\partial v^c}{\partial y_j}\,d\mathbf{y} \;+\; \int_{\Omega_{pc,d}} \alpha\,\frac{\partial\chi^d_{\rm UB,out}}{\partial y_j}\frac{\partial v^d}{\partial y_j}\,d\mathbf{y} \;=\; \int_{\mathcal{U}_c} \frac{\partial v^c}{\partial y_1}\,d\mathbf{y} \;+\; \int_{\Omega_{pc,d}} \alpha\,\frac{\partial v^d}{\partial y_1}\,d\mathbf{y}\,. \tag{21}$$

Problem (21) differs from the original problem (1) in that $\mathcal{U}_c$ and $\overline{W}_{\#,{\rm UB}}(\mathcal{U})$ in the former respectively substitute $\Omega_{pc,c}$ and $Y(\Omega_{pc})$ in the latter.

In view of the previous results for the effective conductivity $k_e$ and lower bound $k_{\rm LB}$, we now write, based on the solution $\chi_{\rm UB,out}$ of the modified problem (21) in $\mathcal{U}$, the quantity $k_{\rm UB}$ as

$$k_{\rm UB} \equiv a_{\Omega_{pc}}(\chi_{\rm UB}) = \min_{w \in W_{\#,{\rm UB}}(\Omega_{pc})} a_{\Omega_{pc}}(w) , \tag{22}$$

which is shown below to be an upper bound for $k_e$. From Eqs. (21)–(22) and (6), and the fact that $J_{\mathcal{D}_{{\rm UB},n}}(\chi_{\rm UB,in}\{\mathbf{y};\overline{C}_n\}) = 0$, $n = 1,\ldots,\mathcal{N}$, $k_{\rm UB}$ can be rewritten as (see details in Machado, 1999)

$$k_{\rm UB} = 1 + (\alpha - 1)c - \frac{1}{|\Omega_{pc}|}\left(\int_{\mathcal{U}_c} \frac{\partial \chi^c_{\rm UB,out}}{\partial y_1}\, d\mathbf{y} + \int_{\Omega_{pc,d}} \alpha \frac{\partial \chi^d_{\rm UB,out}}{\partial y_1}\, d\mathbf{y}\right) . \tag{23}$$

Finally, we now prove mathematically the physically–expected bounding property of $k_{\rm UB}$, by using function space restriction arguments:

$$\begin{aligned} k_{\rm UB} = a_{\Omega_{pc}}(\chi_{\rm UB}) &= \min_{w \in W_{\#,{\rm UB}}(\Omega_{pc})} a_{\Omega_{pc}}(w) \\ &\geq \min_{w \in Y(\Omega_{pc})} a_{\Omega_{pc}}(w) = a_{\Omega_{pc}}(\chi) = k_e , \end{aligned} \tag{24}$$

where $\chi$ is the solution to the original mesoscale problem (1). The inequality (24) follows from the fact that $W_{\#,{\rm UB}}(\Omega_{pc}) \subset Y(\Omega_{pc})$.

## 4. NUMERICAL SOLUTION

Numerical solution of problems (1), (9), and (21) requires three steps: geometry and mesh generation, finite element discretization and solution of the resultant linear system of algebraic equations. Geometry and mesh generation for our thermal composites domains are described in detail in Cruz & Patera (1995), Cruz (1997), and Machado (1999); in this latter reference, the meshing of the nips boundaries is further explained. The finite element discretization procedure to arrive at the discrete problems for $\chi$, $\chi_{\rm LB}$ and $\chi_{\rm UB,out}$ is similar to the one described in Cruz (1997). The main differences required for the treatment of the nips boundaries are: for the lower–bound problem, the appropriate Neumann boundary conditions are naturally enforced; for the upper–bound problem, the constant temperature conditions are enforced by making all the finite–element global nodes on the boundaries of each nip region $\mathcal{D}_{{\rm UB},n}$ to correspond to the same temperature degree–of–freedom, $C_n$, $n = 1,\ldots,\mathcal{N}$. Finally, we choose the well–known conjugate gradient algorithm (Cruz & Patera, 1995; Machado, 1999), with no preconditioning, for iterative solution of the discrete problems.

## 5. RESULTS AND CONCLUSIONS

In this section we present our results for the non–dimensional transverse effective conductivity and associated lower and upper bounds for the square array of fibers; the subscript $h$ is used to indicate all *numerically* calculated quantities. For illustrative purposes, Figure 2 shows two meshes for the square array, generated for $c = 0.75$: the mesh on the left is for domain $\Omega_{pc}$ ($\mathcal{N} = 0$), and the mesh on the right is for both modified domains $\mathcal{L}$ and $\mathcal{U}$ ($\mathcal{N} = 2$); the meshes have been purposedly made coarse around the corners of the square to facilitate visualization (see comment about mesh generation below).

All the results have been brought together in Table 1, where we show: $k_e$, the effective conductivity results of Perrins *et al.* (1979) for the square array; $k_{e,h}$, our numerical results for the effective conductivity; $k_{{\rm LB},h}$ and $k_{{\rm UB},h}$, respectively the lower and upper bound for $k_{e,h}$; $\overline{k}_{e,h}$ and $\overline{E}_r$, respectively the effective conductivity estimate based on the bounds and the associated relative error, given by

$$\overline{k}_{e,h} = \frac{1}{2}\left(k_{{\rm LB},h} + k_{{\rm UB},h}\right) , \tag{25}$$

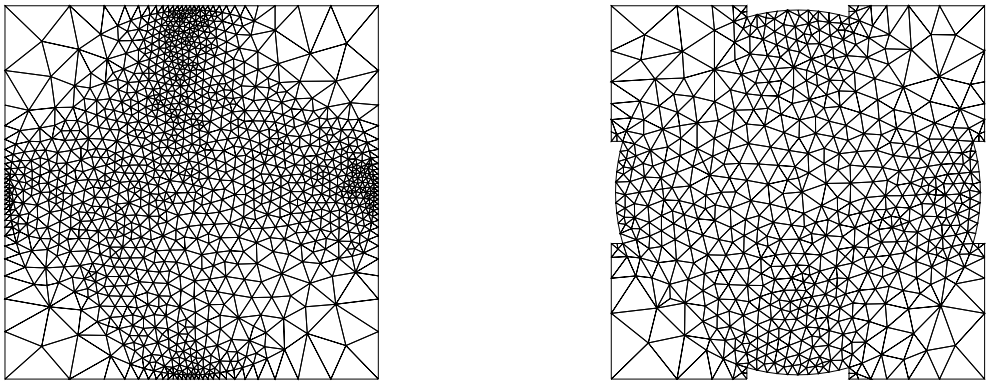

Figure 2: Illustrative finite element meshes for the square array, $c = 0.75$: mesh on the left is for $\Omega_{pc}$ ($\mathcal{N} = 0$), and mesh on the right is for both $\mathcal{L}$ and $\mathcal{U}$ ($\mathcal{N} = 2$).

$$\overline{E}_r \;=\; \frac{(k_{\mathrm{UB},h} - k_{\mathrm{LB},h})/2}{\overline{k}_{e,h}} \times 100\ \%\,. \tag{26}$$

Our numerical results have been obtained using linear triangles; based on previous studies (Cruz & Patera, 1995; Cruz, 1997), we have chosen mesh parameters and conjugate–gradient tolerances so as to guarantee that the discretization error and incomplete–iteration error are small relative to the error associated with the bounds. The results in Table 1 have been grouped in two sets; for both sets, three values of the ratio of phase conductivities, $\alpha \in \{2, 10, 50\}$, and two values of the nip width parameter, $\beta \in \{0.04, 0.06\}$, have been selected. The first set of results, in the top half of Table 1, are obtained for two high concentration values, $c \in \{0.75, 0.78\}$, for which *it is still possible* to generate a mesh in $\Omega_{pc}$ using the procedure described in Cruz (1997). For the first set, the distance $\gamma$ between neighboring fibers is large enough to allow for mesh generation in $\Omega_{pc}$ (Fig. 2); since $\gamma$ has to be smaller than the nip threshold parameter $\gamma_c$ for a pair of fibers to form a nip, we use the artifact of setting $\gamma_c$ to a high enough value when $c \in \{0.75, 0.78\}$. The second set of results, in the bottom half of Table 1, are obtained for two high concentration values, including maximum packing, $c \in \{0.785, \pi/4\}$, for which *it is not possible* to generate a mesh in $\Omega_{pc}$ using the procedure described in Cruz (1997); note Perrins *et al.* (1979) do not provide a value of $k_e$ for maximum packing.

We now make several remarks. First, as expected from the mathematical proofs of previous sections, we note that the hierarchy of the bounds is obtained for all chosen values of $\beta$, $c$ and $\alpha$: $k_{\mathrm{LB},h} < k_{e,h} < k_{\mathrm{UB},h}$ . Second, the gap $\Delta \equiv k_{\mathrm{UB},h} - k_{\mathrm{LB},h}$ gets smaller (i.e., $k_{\mathrm{LB},h}$ increases and $k_{\mathrm{UB},h}$ decreases) as $\beta$ decreases, for all values of $c$ and $\alpha$; we therefore observe, in both sets of results, that the relative error $\overline{E}_r$ decreases as $\beta$ decreases. Third, for the same values of $\alpha$ and $\beta$, the relative error $\overline{E}_r$ decreases as the concentration increases, because the quotient of the area of $\mathcal{L}$ or $\mathcal{U}$ and the area of $\Omega_{pc}$ increases as the concentration increases. Finally, we note that, for the same values of $c$ and $\beta$, the relative error $\overline{E}_r$ increases as the ratio of phase conductivities $\alpha$ increases; for example, at maximum packing with $\beta = 0.04$, we achieve the relative errors of 0.53%, 4.1%, and 26% for $\alpha = 2$, $\alpha = 10$, and $\alpha = 50$, respectively.

We conclude that we have successfully extended the variational–bound nip–element technique of Cruz *et al.* (1995) and Ghaddar (1994) to solve the problem of transverse heat conduction in unidirectional composites with a *thermally–conducting* dispersed phase. We have provided precise error bounds for the effective conductivity at maximum packing for the square array. Future work shall extend the current implementation to calculate the effective conductivity of *random* arrays of fibers, which are more relevant to the study of real materials, and, also, develop anisotropic microscale models to derive sharper bound values for $k_e$ , which, from

the above analysis, are clearly needed for higher values of the ratio of phase conductivities.

Table 1: Effective conductivity results for the square array: semi–analytical, $k_e$ , numerical, $k_{e,h}$ , lower bound, $k_{\mathrm{LB},h}$ , upper bound, $k_{\mathrm{UB},h}$ , conductivity estimate, $\overline{k}_{e,h}$ , and relative error, $\overline{E}_r$ . Parameters: $c \in \{0.75, 0.78, 0.785, \pi/4\}$, $\alpha \in \{2, 10, 50\}$, $\beta \in \{0.04, 0.06\}$.

| $c$ | $\alpha$ | | | | | | | | |
|---|---|---|---|---|---|---|---|---|---|
| | 2 | | | 10 | | | 50 | | |
| 0.75 | $\beta$ | $k_e$ | $k_{e,h}$ | $\beta$ | $k_e$ | $k_{e,h}$ | $\beta$ | $k_e$ | $k_{e,h}$ |
| | | 1.6767 | 1.677 | | 4.9443 | 4.946 | | 9.5355 | 9.546 |
| | 0.06 | $k_{\mathrm{LB},h}$ | $k_{\mathrm{UB},h}$ | 0.06 | $k_{\mathrm{LB},h}$ | $k_{\mathrm{UB},h}$ | 0.06 | $k_{\mathrm{LB},h}$ | $k_{\mathrm{UB},h}$ |
| | | 1.620 | 1.686 | | 4.240 | 5.833 | | 6.793 | 23.61 |
| | | $\overline{k}_{e,h}$ | $\overline{E}_r$ | | $\overline{k}_{e,h}$ | $\overline{E}_r$ | | $\overline{k}_{e,h}$ | $\overline{E}_r$ |
| | | 1.65 | 2.0% | | 5.0 | 16% | | 15 | 56% |
| | 0.04 | $k_{\mathrm{LB},h}$ | $k_{\mathrm{UB},h}$ | 0.04 | $k_{\mathrm{LB},h}$ | $k_{\mathrm{UB},h}$ | 0.04 | $k_{\mathrm{LB},h}$ | $k_{\mathrm{UB},h}$ |
| | | 1.647 | 1.683 | | 4.524 | 5.653 | | 7.714 | 21.77 |
| | | $\overline{k}_{e,h}$ | $\overline{E}_r$ | | $\overline{k}_{e,h}$ | $\overline{E}_r$ | | $\overline{k}_{e,h}$ | $\overline{E}_r$ |
| | | 1.67 | 1.1% | | 5.1 | 11% | | 15 | 47% |
| 0.78 | $\beta$ | $k_e$ | $k_{e,h}$ | $\beta$ | $k_e$ | $k_{e,h}$ | $\beta$ | $k_e$ | $k_{e,h}$ |
| | | 1.7154 | 1.715 | | 5.8037 | 5.805 | | 16.310 | 16.32 |
| | 0.06 | $k_{\mathrm{LB},h}$ | $k_{\mathrm{UB},h}$ | 0.06 | $k_{\mathrm{LB},h}$ | $k_{\mathrm{UB},h}$ | 0.06 | $k_{\mathrm{LB},h}$ | $k_{\mathrm{UB},h}$ |
| | | 1.671 | 1.719 | | 4.983 | 6.126 | | 9.575 | 24.66 |
| | | $\overline{k}_{e,h}$ | $\overline{E}_r$ | | $\overline{k}_{e,h}$ | $\overline{E}_r$ | | $\overline{k}_{e,h}$ | $\overline{E}_r$ |
| | | 1.70 | 1.4% | | 5.6 | 10% | | 17 | 44% |
| | 0.04 | $k_{\mathrm{LB},h}$ | $k_{\mathrm{UB},h}$ | 0.04 | $k_{\mathrm{LB},h}$ | $k_{\mathrm{UB},h}$ | 0.04 | $k_{\mathrm{LB},h}$ | $k_{\mathrm{UB},h}$ |
| | | 1.695 | 1.717 | | 5.369 | 6.004 | | 11.76 | 22.96 |
| | | $\overline{k}_{e,h}$ | $\overline{E}_r$ | | $\overline{k}_{e,h}$ | $\overline{E}_r$ | | $\overline{k}_{e,h}$ | $\overline{E}_r$ |
| | | 1.71 | 0.64% | | 5.7 | 5.6% | | 17 | 33% |
| 0.785 | $\beta$ | $k_e$ | $k_{e,h}$ | $\beta$ | $k_e$ | $k_{e,h}$ | $\beta$ | $k_e$ | $k_{e,h}$ |
| | | 1.7220 | — | | 6.004 | — | | 20.5 | — |
| | 0.06 | $k_{\mathrm{LB},h}$ | $k_{\mathrm{UB},h}$ | 0.06 | $k_{\mathrm{LB},h}$ | $k_{\mathrm{UB},h}$ | 0.06 | $k_{\mathrm{LB},h}$ | $k_{\mathrm{UB},h}$ |
| | | 1.680 | 1.724 | | 5.16 | 6.19 | | 10.5 | 24.9 |
| | | $\overline{k}_{e,h}$ | $\overline{E}_r$ | | $\overline{k}_{e,h}$ | $\overline{E}_r$ | | $\overline{k}_{e,h}$ | $\overline{E}_r$ |
| | | 1.70 | 1.3% | | 5.7 | 9.0% | | 18 | 41% |
| | 0.04 | $k_{\mathrm{LB},h}$ | $k_{\mathrm{UB},h}$ | 0.04 | $k_{\mathrm{LB},h}$ | $k_{\mathrm{UB},h}$ | 0.04 | $k_{\mathrm{LB},h}$ | $k_{\mathrm{UB},h}$ |
| | | 1.704 | 1.723 | | 5.59 | 6.08 | | 13.5 | 23.3 |
| | | $\overline{k}_{e,h}$ | $\overline{E}_r$ | | $\overline{k}_{e,h}$ | $\overline{E}_r$ | | $\overline{k}_{e,h}$ | $\overline{E}_r$ |
| | | 1.713 | 0.55% | | 5.8 | 4.2% | | 18 | 27% |
| $\pi/4$ | $\beta$ | $k_e$ | $k_{e,h}$ | $\beta$ | $k_e$ | $k_{e,h}$ | $\beta$ | $k_e$ | $k_{e,h}$ |
| | | — | — | | — | — | | — | — |
| | 0.06 | $k_{\mathrm{LB},h}$ | $k_{\mathrm{UB},h}$ | 0.06 | $k_{\mathrm{LB},h}$ | $k_{\mathrm{UB},h}$ | 0.06 | $k_{\mathrm{LB},h}$ | $k_{\mathrm{UB},h}$ |
| | | 1.681 | 1.725 | | 5.18 | 6.19 | | 10.6 | 24.9 |
| | | $\overline{k}_{e,h}$ | $\overline{E}_r$ | | $\overline{k}_{e,h}$ | $\overline{E}_r$ | | $\overline{k}_{e,h}$ | $\overline{E}_r$ |
| | | 1.70 | 1.3% | | 5.7 | 8.9% | | 18 | 40% |
| | 0.04 | $k_{\mathrm{LB},h}$ | $k_{\mathrm{UB},h}$ | 0.04 | $k_{\mathrm{LB},h}$ | $k_{\mathrm{UB},h}$ | 0.04 | $k_{\mathrm{LB},h}$ | $k_{\mathrm{UB},h}$ |
| | | 1.705 | 1.723 | | 5.61 | 6.09 | | 13.7 | 23.3 |
| | | $\overline{k}_{e,h}$ | $\overline{E}_r$ | | $\overline{k}_{e,h}$ | $\overline{E}_r$ | | $\overline{k}_{e,h}$ | $\overline{E}_r$ |
| | | 1.714 | 0.53% | | 5.9 | 4.1% | | 18 | 26% |

*Acknowledgements*

M. E. C. and L. B. M. would like to gratefully acknowledge the support of the Brazilian Council for Development of Science and Technology (CNPq) through Grant 521002/97–4, FAPERJ through Grant E–26/150.654/97, CAPES through the M.Sc. stipend of L.B.M., and the Cray time provided by NACAD/COPPE/UFRJ.

## REFERENCES

Ayers, G. H. & Fletcher L. S., 1998, Review of the Thermal Conductivity of Graphite–Reinforced Metal Matrix Composites, Journal of Thermophysics and Heat Transfer, vol. 12, pp. 10–16.

Cruz, M. E., 1997, Two–Dimensional Simulation of Heat Conduction in Ordered Composites With a Thermally–Conducting Dispersed Phase, Proceedings of the 14th COBEM, Paper COB288, Bauru, SP, Brazil.

Cruz, M. E., Ghaddar, C. K. & Patera A. T., 1995, A Variational–Bound Nip–Element Method for Geometrically Stiff Problems; Application to Thermal Composites and Porous Media, Proc. R. Soc. Lond. A, vol. 448, pp. 1–30.

Cruz, M. E. & Patera, A. T., 1995, A Parallel Monte–Carlo Finite–Element Procedure for the Analysis of Multicomponent Random Media, Int. J. Numer. Methods Engng., vol. 38, pp. 1087–1121.

Furmañski P., 1997, Heat Conduction in Composites: Homogenization and Macroscopic Behavior, Appl. Mech. Rev., vol. 50, pp. 327–356.

Ghaddar, C. K., 1994, Parallel Analytico–Computational Methods for Multicomponent Media: Application to Thermal Composites and Porous Media Flows, Ph.D. Thesis, Massachusetts Institute of Technology.

Hasselman, D. P. H., Johnson, L. F., Syed, R., Taylor, M. P. & Chyung K., 1987, Heat Conduction Characteristics of a Carbon–Fibre–Reinforced Lithia–Alumino–Silicate Glass–Ceramic, J. Mater. Sci., vol. 22, pp. 701–709.

Machado, L. B., 1999, Calculation of the Effective Conductivity of Unidirectional Composites, M.Sc. Thesis (in Portuguese), PEM/COPPE/UFRJ.

Perrins, W. T., McKenzie, D. R. & McPhedran, R. C., 1979, Transport properties of regular arrays of cylinders, Proc. R. Soc. Lond. A, vol. 369, pp. 207–225.

Pilling, M. W., Yates, B., Black, M. A. & Tattersall P., 1979, The Thermal Conductivity of Carbon Fibre–Reinforced Composites, J. Mater. Sci., vol. 14, pp. 1326–1338.

Sangani, A. S. & Yao, C., 1988, Transport processes in random arrays of cylinders. I. Thermal conduction, Phys. Fluids, vol. 31, pp. 2426–2434.

Torquato, S., 1991, Random heterogeneous media: Microstructure and improved bounds on effective properties, Appl. Mech. Rev., vol. 44, pp. 37–76.

Tzou, D. Y., 1991, A Universal Model for the Overall Thermal Conductivity of Porous Media, J. Comp. Mat., vol. 25, pp. 1064–1084.